© 2017. Published by The Company of Biologists Ltd | Journal of Experimental Biology (2017) 220, 1663-1673 doi:10.1242/jeb.153379

RESEARCH ARTICLE

Waveform sensitivity of electroreceptors in the pulse-type weakly electric fish *Gymnotus omarorum*

Alejo Rodríguez-Cattaneo, Pedro A. Aguilera and Angel A. Caputi*

ABSTRACT

As in most sensory systems, electrosensory images in weakly electric fish are encoded in two parallel pathways, fast and slow. From work on wave-type electric fish, these fast and slow pathways are thought to encode the time and amplitude of electrosensory signals, respectively. The present study focuses on the primary afferents giving origin to the slow path of the pulse-type weakly electric fish *Gymnotus omarorum*. We found that burst duration coders respond with a high-frequency train of spikes to each electric organ discharge. They also show high sensitivity to phase-frequency distortions of the self-generated local electric field. We explored this sensitivity by manipulating the longitudinal impedance of a probe cylinder to modulate the stimulus waveform, while extracellularly recording isolated primary afferents. Resistive loads only affect the amplitude of the re-afferent signals without distorting the waveform. Capacitive loads cause large waveform distortions aside from amplitude changes. Stepping from a resistive to a capacitive load in such a way that the stimulus waveform was distorted, without changing its total energy, caused strong changes in latency, inter-spike interval and number of spikes of primary afferent responses. These burst parameters are well correlated suggesting that they may contribute synergistically in driving downstream neurons. This correlation also suggests that each receptor encodes a single parameter in the stimulus waveform. The finding of waveform distortion sensitivity is relevant because it may contribute to: (a) enhance electroreceptive range in the peripheral 'electrosensory field', (b) a better identification of living prey at the 'foveal electrosensory field' and (c) detect the presence and orientation of conspecifics. Our results also suggest a revision of the classical view of amplitude and time encoding by fast and slow pathways in pulse-type electric fish.

KEY WORDS: Electroreception, Electric color, Peripheral coding, Electric image

INTRODUCTION

Electric fish use an active electric sense for the evaluation of nearby objects. A self-generated electric field is modified by the impedance and geometry of nearby objects. The resulting changes in the transcutaneous electric field are transduced by cutaneous electroreceptors and encoded as train of spikes in primary electroreceptive afferents (Bullock et al., 1961; Fessard and Szabo, 1961; Lissmann, 1958; Szabo and Fessard, 1974; Wright, 1958). This information is further processed in the brain stem (Aumentado-Armstrong et al., 2015; Bell and Maler, 2005; Heiligenberg and Rose, 1985; Kawasaki, 2005) and telencephalon (Harvey Girard et al., 2010; Trinh et al., 2016), giving origin to reflex (Caputi et al., 2003; Post and von der Emde, 1999), stereotyped (Heiligenberg, 1991; Kawasaki, 2005; Moller, 1995) and learned behaviors (Jun et al., 2014; Schumacher et al., 2016; Walton and Moller, 2010).

Electric fish of the families Apteronotidae, Eigenmannidae and Sternopygidae from America and Gymnarchidae from Africa emit a continuous sinewave-like signal with a very sharp power spectral density. These taxa are called 'wave fish' (Coates et al., 1954). Conversely, the families Mormyridae, Rhamphychtydae, Hypopomidae and Gymnotidae emit a repetitive brief wavelet-like pulse separated by intervals several times longer than the pulse duration. These are called 'pulse fish' (Coates et al., 1954). These two strategies of object 'illumination' give origin to correspondingly different strategies of image encoding and processing (Dye and Meyer, 1986).

Wave fish electroreceptors encode the zero crossing time and amplitude of the self-generated local stimuli (referred to here as self-generated local electric organ discharge, sLEOD) using two types of receptors which are respectively called T and P units in wave-type gymnotiforms and S and O in mormyriforms (Scheich and Bullock, 1974; Zakon, 1986). While T and S units fire a single spike phase locked with many but not all zero crossing of the sLEOD (Heiligenberg, 1991), P and O units are characterized by a probability of firing proportional to the amplitude of the local signal (Benda et al., 2005, 2006; Chacron et al., 2000, 2005; Clarke et al., 2015; Kawasaki, 2005).

Electroreceptors of pulse fish also encode the sLEOD using two types of receptors, which are respectively called pulse markers and burst duration coders in gymnotiforms, and knollenorgan and mormyromast receptors in mormyriforms (Kawasaki, 2005; Szabo, 1974; Zakon, 1986). Pulse markers and knollenorgans fire a single spike, phase locked to every sLEOD and encode the amplitude of the sLEOD as small changes in latency (Bell and Grant, 1989; Castello et al., 1998; Szabo and Fessard, 1974). These electroreceptors give origin to the so-called 'fast electrosensory pathways' (Szabo et al., 1975). Burst duration coders and mormyromast receptors fire short but high-frequency trains of spikes phase locked with the sLEOD and encode changes in amplitude (Bastian, 1976, 1977; Bell, 1990a,b; Hagiwara and Morita, 1963; McKibben et al., 1993; Sawtell et al., 2006; Watson and Bastian, 1979; Yager and Hopkins, 1993). These electroreceptors give origin to the so-called 'slow electrosensory pathways' (Szabo et al., 1975).

While mormyromasts are complex organs, having two chambers housing two different receptor cell populations innervated by different fibers (Bell et al., 1989; Szabo, 1974), burst duration coders have a single chamber with a single population of cells

Departamento de Neurociencias Integrativas y Computacionales, Instituto de Investigaciones Biológicas Clemente Estable, Av. Italia 3318, C.P 11600, Montevideo, Uruguay.

*Author for correspondence (acaputi@iibce.edu.uy)

A.A.C., 0000-0002-7238-0538

Received 28 November 2016; Accepted 13 February 2017

Journal of Experimental Biology (2017) 220, 1663-1673 doi:10.1242/jeb.153379

innervated by a single fiber (Caputi et al., 2002; Echagüe and Trujillo-Cenóz, 1980; Szabo, 1974).

The two fiber types originating in the different chambers of mormyromast receptors encode the sLEOD differently. Type A fibers, originating in the outer chamber, encode amplitude (Bell, 1990a,b), whereas type B fibers, originating in the inner chamber, encode both the amplitude and the waveform of the sLEOD (von der Emde and Bleckmann, 1992; von der Emde and Bell, 1994). The ability to measure separately the amplitude and waveform of the stimulus allows the fish to identify both object resistance and capacitance, respectively (Meyer, 1982; von der Emde, 1990; von der Emde and Ronacher, 1994). This process may be likened to sensitivity in the retina to different wavelengths of light, suggesting the metaphor of 'electrical color' in electrosensory systems (Budelli and Caputi, 2000).

In pulse gymnotiforms, the primary afferents referred to as burst duration coders were initially subclassified according to their response to short sinewave bursts as low pass, wide band and narrow band units (Bastian, 1976, 1977; Watson and Bastian, 1979). The differences between low pass and wide band were not so clear in subsequent reports (McKibben et al., 1993; Yager and Hopkins, 1993). These differences in responsiveness are important as the electric field generated by pulse gymnotiforms is the weighted sum of multiple electrocytes discharging sequentially along the length of the body, each having a different timing, waveform and amplitude (Caputi et al., 1989, 1994, 1998a; Rodríguez-Cattáneo et al., 2008, 2013). Spatiotemporal heterogeneity in electrocyte discharges results in regionally specific local fields 'illuminating' the objects in the surrounding water (Assad et al., 1999; Aguilera et al., 2001; Castelló et al., 2009; Pedraja et al., 2014). As a consequence, at all points of the skin with the exception of the foveal region, i.e. the perioral region at the anterior tip of the fish's body (Aguilera et al., 2001; Castello et al., 2000), the basal stimulus waveform is site specific. Conversely, because the rostral pole is relatively farther from the electric organ, the entire foveal region receives a similar stimulus waveform in the absence of objects (Caputi and Budelli, 1995; Castello et al., 2000; Aguilera et al., 2001). In fact, changes in the waveform of the foveal sLEOD that do not affect the total energy of the stimulus signal (as measured by its root mean squared value, rms) are detected by the fish, as shown by strong novelty responses in *Gymnotus omarorum* to changes in waveform only (reported as *Gymnotus carapo* in Aguilera and Caputi, 2003). In addition, electroreceptor modeling showed the possibility that these receptors were able to respond differently to capacitive and resistive objects (Cilleruelo and Caputi, 2012). However, to the extent of our knowledge, the effect of changes in sLEOD waveform on primary afferent responses themselves has not been well examined in pulse gymnotiforms.

This study extends our previous work on waveform encoding in the pulse gymnotiform *Gymnotus omarorum* Richer-de-Forges, Crampton and Albert 2009, using objects with capacitive impedance (Aguilera and Caputi, 2003; Cilleruelo and Caputi, 2012). We compared in non-anesthetized and non-curarized self-discharging fish the response of burst duration coders to probe objects having resistive or capacitive impedance that changed the sLEOD amplitude and waveform over a wide range. Comparison of responses to capacitive and resistive loads of the same amplitude shows that burst duration coders respond more strongly to changes in the waveform than to changes in the total energy of the stimulus.

MATERIALS AND METHODS

Experimental procedures

Six *G. omarorum*, 24.5±3.9 cm in length, of undetermined sex were used following the guidelines of the CHEA (Comisión Honoraria de Experimentación Animal, ordinance 4332-99, Universidad de la República Oriental del Uruguay). Experiments were approved by the Animal Ethics Committee of the Instituto de Investigaciones Biológicas Clemente Estable (protocol number 001/03/2011). Fish were gathered at Laguna del Cisne (Maldonado, Uruguay) 1–4 months before the experiment, kept in individual aquaria under a natural light cycle and fed with insect larvae.

Decerebration and surgical procedures

All physiological experiments were performed in decerebrated fish (Pereira et al., 2014). Decerebrated fish continued to breathe and move the anal fin, showed electric organ discharge (EOD) at a constant rate similar to that observed in intact fish and responded to electrosensory and other sensory stimuli with transient accelerations (i.e. novelty responses). Surgical procedures were conducted with the fish under deep anesthesia (Eugenol 100 mg l^{-1} in the aquarium water; Neiffer and Stamper, 2009). Once the fish stopped discharging, the skin over the upper cranial projection of the brain was removed and two small holes were drilled on the skull over the forebrain, one on each side of the midline. A small vacuum aspiration nozzle was introduced through one of the holes to completely remove the forebrain. Once decerebration was complete, the fish was moved into the recording chamber and anesthesia removed. The chamber consisted of a 26×45 cm tank filled to a depth of 6 cm with aquarium water (100 µS cm^{-1}) mounted on a vibration isolation table. A thin nichrome wire (150 µm diameter) was passed through both holes and the skull was firmly attached to a wood holder. These wires were then embedded in a dental cement structure binding the skull and the holder. A cotton thread was passed along the dorsal muscular mass, leaving the body at about 5 cm from the tip of the tail. Using this thread, firmly attached to the head holder and a caudal support, we positioned the fish body straight along the long axis of the tank. Then, we removed a 2×2 mm square portion of skull bone over the electrosensory lateral line lobe (ELL) taking care to maintain the water level below the border of the wound and above the mouth opening. Spontaneous EODs resumed during this fixation procedure or shortly thereafter.

Electrophysiological recordings

The experimental procedure is illustrated in Fig. 1A. Extracellular unitary activity was recorded between a reference electrode placed at the cisterna magna and active electrodes inserted in the deep layers of the ELL. For ELL recordings, we used a 'Michigan type' multitrode with 16 channels distributed along a line 50 µm apart. Recordings were made using a multiplexed differential amplifier (A-M systems 3600, gain ranging between 5000 and 20,000 adjusted during the experiment). We adjusted the low and high cut-off frequencies of the band-pass filters (second-order Butterworth) to 300 kHz at the low end and 5 kHz at the high end, in order to select electroreceptor unitary activity.

We modulated the sLEOD by moving objects (metal or plastic cylinders 1 cm diameter and 3 cm axis oriented vertically) over the body surface to find the center of the receptive field. The vertical cylinder was manually moved along the skin attached at the end of the arm of an XY plotter (Hewlett-Packard 7015A) in order to measure its position along the skin. Once we found the best stimulation place, we tested properties of the receptor using an active cylindrical probe similar to that used in previous experiments comparing fish responsiveness to capacitive and resistive objects (Aguilera and Caputi, 2003; Caputi et al., 2003; von der Emde, 1990). The active cylindrical probe (3 mm diameter, 2 cm length) consisted of a plastic tube with two carbon plugs at its ends oriented

Journal of Experimental Biology

Journal of Experimental Biology (2017) 220, 1663-1673 doi:10.1242/jeb.153379

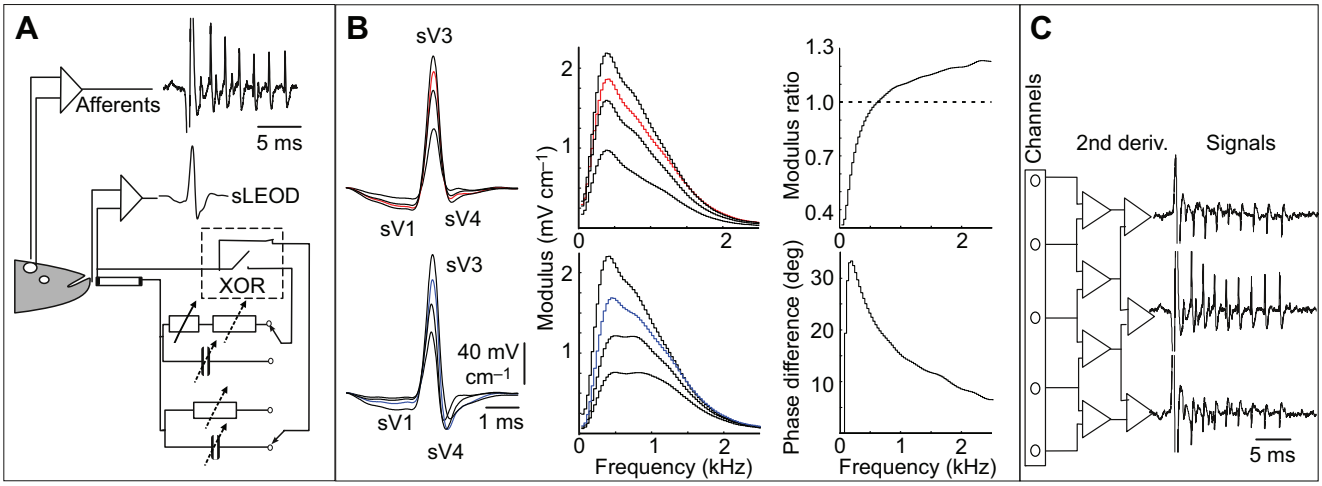

Fig. 1. Experimental setup, stimulus manipulation and digital preprocessing. (A) Analog recordings. The unitary activity of primary afferents was recorded at the entrance to the brain of the anterior lateral line nerve, and the local stimulus in front of the receptor was recorded when the electrosensory image was modulated by changing the load of a probe object consisting of a plastic tube with carbon plugs at its ends. A computer triggered an 'exclusive or' switch (XOR) to make a step between pairs of impedance values including capacitance and resistance. (B) Phase-frequency distortion of self-generated local electric organ discharge (sLEOD) is shown by comparing resistive (top) and capacitive (bottom) effects. In the left and middle panels, the effects of four resistance (270, 54, 10 and 1 kΩ) and four capacitance (2.3, 4.8, 10 and 33 nF) values are represented. The colored traces indicate the responses to two loads (blue: 10 nF; red: 10 kΩ) in which the total energy was matched but different waveforms occur. The right panels compare the amplitude (modulus ratio) and phase spectra (phase difference) of the fast Fourier transform (FFT) of the blue and red traces. Left: while local stimuli caused by resistive objects show major changes in amplitude but only small changes in waveform, those resulting from capacitive objects cause, besides the changes in amplitude, large changes in waveform consisting of a reduction of sV1 and an increase of sV4. Middle: FFT component modulus as a function of frequency for the same traces. Capacitance increases the relative weight of larger frequency components in total energy. Right, top: ratio between moduli of the signals marked with blue (10 nF capacitance) and red (10 kΩ resistance) showing that frequency components larger than 600 Hz are better represented when the object load is capacitive. Right, bottom: phase difference between the signals marked with blue (10 nF capacitance) and red (10 kΩ resistance), showing that there is a large difference for low frequencies and a gradual reduction in this difference as frequency increases. (C) Digital processing. Afferent spikes were recorded with a multitrode (16 channels; left) and the second spatial derivative was calculated digitally (middle) to increase the signal to noise ratio. Signals (right) were converted into point processes.

perpendicularly to the skin. A pair of wires connected these carbon electrodes and allowed us to control the longitudinal impedance of the object and consequently the stimulus waveform. The loading elements (resistors 270, 54, 20, 10 and 1 kΩ or capacitors 2.2, 3.3, 4.8, 10 and 33 nF) were selected manually for long-lasting steps or using a computer-triggered switch in order to study the transition between responses caused by two different loads. A previous study (Aguilera and Caputi, 2003) indicated the range of capacitance in which phase-frequency distortions occur (Fig. 1B). Beyond the limits of 1 and 50 nF, the sLEODs appeared identical to open and short circuit signals. It is important to note that single capacitors cause the largest possible waveform distortions (Aguilera and Caputi, 2003).

The sLEOD in front of the probe was measured as the voltage drop between the bare tip of a 100 µm diameter insulated copper wire placed against the skin and the carbon base of the stimulus-object cylinder nearest to the fish (2 mm separation). The total energy of the stimulus was measured as the root mean squared value of the sLEOD (rms sLEOD). The sLEOD of *G. omarorum* has three main deflections at the foveal region (called components or phases in other studies and referred to as sV1, sV3 and sV4 according to the nomenclature of Trujillo-Cenóz et al., 1984, extended by Castello et al., 2000 and Aguilera et al., 2001). These deflections were differentially modified by resistive and capacitive loads. When the resistance of the probe object increased, the rms sLEOD decreased and the waveform remained similar with a small decrease in sV4 (Fig. 1B). Besides evoking changes in rms sLEOD, capacitors caused important changes in waveform consisting of reductions of the early negative component (sV1) and increases of the late negative component (sV4; Fig. 1B). These changes were described previously (Aguilera and Caputi, 2003) and represent a form of phase-frequency distortion of the EOD waveform. In the frequency domain, this distortion is characterized by an increase of the relative weight and an advance in phase of the higher frequency components (Fig. 1B).

The head-to-tail EOD (htEOD), recorded with electrodes placed at the edges of the tank along the fish major body axis, was used as a time reference. These signals were amplified (×100, model 1800 A-M Systems) and second-order Butterworth band-pass filtered (10–10,000 Hz) for observation of individual LEOD waveforms using a digital oscilloscope. All signals were digitized at a minimum of 20 kHz per channel (DataWave Technologies).

Analysis of the activity of the electroreceptor units

During the experiment, we identified afferent fibers through their distinctive property of firing a burst in phase with every EOD. This characteristic differentiates the units located at the deep layers from upper neurons that fire sparsely, once every two or three EODs. In the deep layers we found three types of units. (1) Burst duration coders fire a burst of spikes modulated in latency, intraburst interval and number of spikes by the presence of objects (Bastian, 1977). (2) Pulse markers fire a single spike with a short latency (about 2 ms) modulated by the objects; we could isolate only one of these spikes from the large field potentials integrating the activity of the afferents and spherical cells of the fast electrosensory pathway (Szabo et al., 1975; Castello et al., 1998). (3) Single spiking neurons firing between 4 and 6 ms after the EOD and poorly modulated by ipsilateral and also contralateral stimuli. As these units probably correspond to ovoid and multipolar deep inhibitory cells, here we focus only on the first and second types of units corresponding to primary afferents.

Journal of Experimental Biology (2017) 220, 1663-1673 doi:10.1242/jeb.153379

Spike sorting was done with DataWave SciWorks software (version 8.0). In order to separate the target spike from the field potential and nearby spiking units, we calculated the vertical spatial second derivative of the recorded signals by applying the formula (Fig. 1C):

$$\text{Spatial second derivative} = (\text{upper signal} + \text{lower signal} - 2 \times \text{local signal}).$$

Spikes observed in these transformed signals were selected first using a voltage and time window discriminator; primary sorted spikes were displayed in three contiguous channels to verify that sources and sinks were the same for all selected waveforms and the best parameters for discriminating between different waveforms were defined ad hoc for each unit. Sorting parameters most frequently included (a) amplitude of the maximal (peak) and minimal (valley) values, (b) peak-to-valley amplitudes, (c) peak-to-valley interval and (d) rising and falling slopes. Among the recorded units that were unequivocally identified by their consistent waveforms, we selected those showing a firing pattern consistent with that described for burst duration coders (Bastian, 1976; McKibben et al., 1993). Two main indicators were used to define the unit as a burst duration coder: a high-frequency train firing one-to-one with the EOD and a modulation of the train parameters by a metal object. Finally, we selected the time stamps of 25 units showing enough recording time and experimental maneuvers to answer the questions posed in this study. These time stamp series were used to construct post-EOD raster plots and post-EOD histograms using Octave routines available upon direct request from the corresponding author (A.A.C.).

We characterized the post-EOD bursts by measuring the following parameters: latency of the first spike, first interspike interval and (in the case of stationary data) number of spikes per EOD.

RESULTS

Primary afferent pattern of discharge in the absence and presence of objects

A large field potential corresponding to the synchronized activity of pulse markers and spherical cells of the ELL was usually recorded about 2 ms after the positive peak of the htEOD (Fig. 2A, top). This large field potential precluded the recording of unitary activity of pulse markers except in one case. In this case, the afferent fired a single spike almost phase locked 1.62 ms after the EOD and showing small jitter in latency (s.d. 0.1 ms).

We recorded 25 burst duration coders that responded to the sLEOD in the absence of objects with a high-frequency (200–500 Hz) train of 2–6 spikes, starting between 3.5 and 4.5 ms (3.82±0.76 ms, mean±s.d. of 18 units) after the positive peak of the

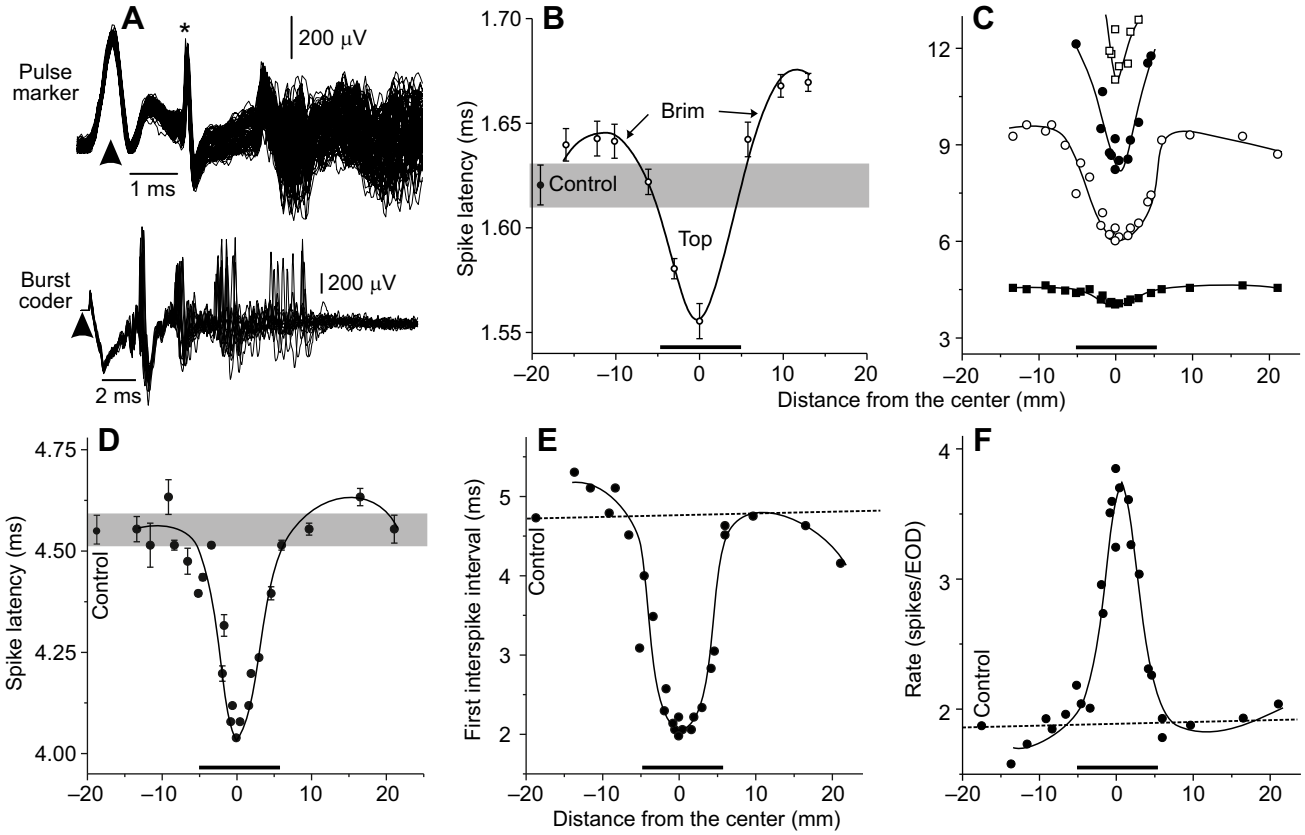

Fig. 2. Comparison between afferents of the fast and slow pathways. (A) Superimposed afferent recordings from two units recorded in different tracks in the same fish. Top: 100 superimposed traces showing the regularity and early latency of a pulse marker response to the electric organ discharge (EOD). Note that the isolated spike (*) precedes the asynchronous mix of action potentials corresponding to the rest of the afferent responses. Bottom: 10 superimposed traces showing the more variable response of the burst duration coders to the EOD. Latencies of the spikes were measured from the maximum of the head-to-tail EOD (htEOD, arrowheads). (B) Receptive field of the pulse marker shown in A. Note the center–peripheral opposition of the receptive field [vertical bars: 2 s.e. around the mean (95% confidence interval); horizontal bar: object diameter]. (C) Receptive field of the burst duration coder afferent shown in A. Each symbol corresponds to the latency of an ordinal spike (filled squares: first spike; open circles: second; filled circles: third; open squares: fourth). (D–F) Parameters of burst duration coder primary afferents as a function of distance from the center of the receptive field. Details as for the pulse marker.

Journal of Experimental Biology

Journal of Experimental Biology (2017) 220, 1663-1673 doi:10.1242/jeb.153379

htEOD (about 7.2 ms after pacemaker firing), and lasting from 4 to 10 ms. The first spike usually had a larger amplitude than the second and this second spike was smaller than the others (Fig. 2A, bottom, and Fig. 3A, a phenomenon also observed in Yager and Hopkins, 1993). The first spike always discharged one-to-one with the EOD and the mean number of spikes per EOD was 2.68 in the absence of objects. The latency of each spike in the train increased in absolute value, variability and proportion of failures as a function of its ordinal number (Fig. 2A, bottom).

The receptive fields showed a 'Mexican hat' profile (with an excitation at the top region and a firing reduction at the brim region) when explored with a metal cylinder (1 cm diameter, 3 cm length placed with the rotation axis vertically) placed 1 mm from the skin. This response function results from a pre-receptor Laplacian filter, which was theoretically and experimentally described in previous papers (Budelli and Caputi, 2000; Caputi et al., 1998b, 2002; Gómez et al., 2004; Caputi et al., 2011; Sanguinetti-Scheck et al., 2011; Pedraja et al., 2014).

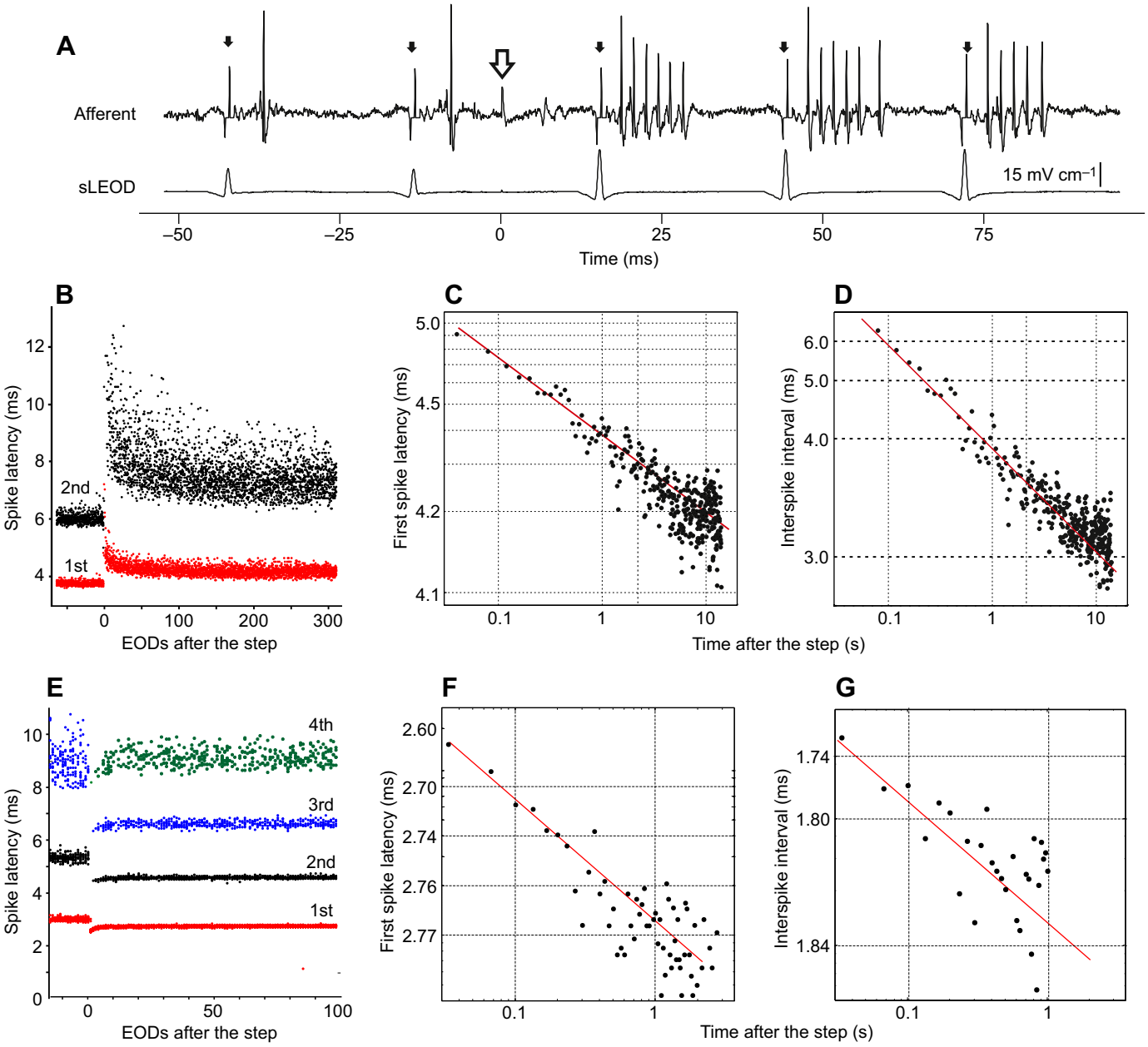

Fig. 3. Spike firing adaptation in three primary afferents. (A) Top: raw data showing the response of a primary afferent when the stimulus probe load was changed from 2.5 MΩ to 1 kΩ. Small arrows indicate the EOD artifacts after second spatial derivative calculation. The stimulus step occurs at time zero, where the large arrow indicates the stepping artifact enhanced by calculation of the second derivative. Note the increase in latency and interspike interval and the decrease in spike number. Bottom: the sLEOD. (B) Ten superimposed raster plots showing the latency adaptation of the first and second spike after a stimulus step from large to small stimulus amplitude. (C) Average latency of the first spike of B across the 10 trials as a function of average timing of each EOD after the step. (D) Average interval between the first and second spikes in B as a function of average timing of each EOD after the step. (E) Ten superimposed raster plots showing the latency adaptation of the first four spikes after a stimulus step from small to large stimulus amplitude. (F) Average latency of the first spike in E as a function of average timing of each EOD after the step. (G) Average interval between the first and second spikes in E as a function of average timing of each EOD after the step. A, B–D and E–G correspond to three different primary afferents.

Journal of Experimental Biology

Journal of Experimental Biology (2017) 220, 1663-1673 doi:10.1242/jeb.153379

In pulse markers, the latency reached a minimum at the center of the receptive field and increased in the periphery. The effect of changing object position was a modulation of spike latency as an important fraction of the control value. Although this modulation was a fraction of a millisecond, there was a significant departure from the control value plus the jitter (Fig. 2B).

Responses of burst duration coders were strongly modulated by the presence of objects. When a metal object was in front of the receptor within a distance equivalent to its radius, the intensity of the burst (i.e. intra-burst frequency and total number of spikes) was larger than the control. At the center of the receptive field, the number of spikes was maximal and their latencies were minimal (Fig. 2C). In the receptive field periphery and also close to the gills (data not shown), the opposite effects were observed. Plastic objects of the same shape and orientation provoked an inverted pattern of modulation (decreased at the center and increased at the periphery). Fig. 2D–F illustrates the average values in steady-state conditions when the object was stepped along a horizontal trajectory.

Three parameters were used to characterize the responses of burst duration coders: (1) the latency of the first spike, (2) interspike intervals during the burst and (3) the number of spikes per EOD. We used the latency of the first spike of the burst and the interval between the first and second spikes because these two parameters were the most constant throughout the stimulus range. The number of spikes was correlated with them. It is important to note that the last spike showed a low firing probability and large variations in latency. Therefore, burst duration does not appear to be the most reliable parameter to carry stimulus information.

Differential responses of burst duration coders to changes in sLEOD

In order to modify both the amplitude and waveform of the local stimulus and compare the relative effects of these variables on receptor responsiveness, we used a probe consisting of a plastic cylindrical tube with two carbon plugs at the ends. The longitudinal impedance of the probe was controlled by connecting a loading element between the two carbon plugs (either a resistor or a capacitor, Fig. 1A). The stimulus sLEOD energy was evaluated by its rms value within a time window of 6 ms (rms sLEOD), and its waveform as the ratio between the negative and positive components (sV1/sV3 and sV4/sV3).

Stepping between pairs of resistive loads caused an abrupt change in the latency of the first spike, the intervals within the burst and the number of spikes. This effect was maximal at the very first EOD after the step (Fig. 3A) and showed fast adaptation in the three parameters (Fig. 3B–G).

The time course of adaptation was well fitted by a hyperbolic function (Fig. 3B–D). This suggests that spike frequency adaptation occurs as in wave gymnotiforms (Benda et al., 2005; Clarke et al., 2014). In addition, for a similar latency, later spikes in the sequence were less variable. This can be observed in Fig. 3E by comparing the mean and variance of the latencies of the last spikes in the sequence before and after the step (i.e. blue versus green dots in the third- and fourth-order spikes, respectively).

When the object probe was loaded at the lowest resistance (1 kΩ), the rms sLEOD increased up to 3 times compared with the value when the object probe was loaded with the largest resistance (2.5 MΩ). The waveform of the sLEOD was a little distorted, showing small increases in sV4 correlated with the increase in rms sLEOD. Conversely, when the probe was loaded with a capacitor, the waveform of the sLEOD showed a marked distortion, consisting of a reduction of the early negative component (sV1) and an increase of the late negative component (sV4; Figs 1, 4–7).

While the responses to resistive loads show monotonic changes in first spike latency, first interspike interval and spikes per EOD, the responses to capacitive loads showed a maximal response at intermediate values. Fig. 4 illustrates the response of a primary afferent when the load of the object probe was stepped along a series of capacitance values. For capacitance values lower than 3.3 nF, sLEOD waveform distortion (i.e. sV4/sV1 ratio) and rms sLEOD as well as receptor responses increased together. Beyond this point, rms sLEOD increased but waveform distortion decreased. However, responses continued to increase up to 10 nF. The 33 nF capacitor provoked the maximum rms sLEOD but showed the smallest waveform distortion. This weaker effect on waveform explains the weaker receptor response.

For most capacitive loads, the responses were stronger than those evoked by resistive loads causing similar changes in the rms

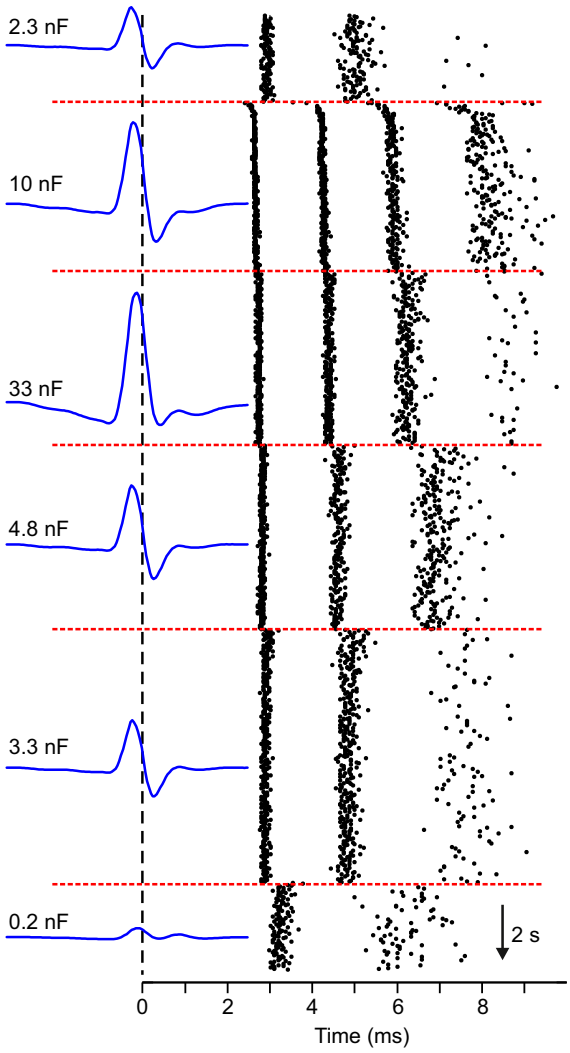

Fig. 4. Responses of burst duration coders to capacitance. The raster plots (right) show the waveform of a single experiment in which the stimulus probe was sequentially loaded with capacitors of different values using a rotating switch. Each step is marked by a horizontal red line. The corresponding stimulus traces (left) show the changes in amplitude and waveform (blue) corresponding to each value of capacitance, aligned by a common timing reference (the positive peak of the htEOD, dashed line). Note that the largest capacitor (33 nF) causing the largest sLEOD stimuli generates a less intense response than a smaller capacitor (10 nF).

Journal of Experimental Biology

Journal of Experimental Biology (2017) 220, 1663-1673 doi:10.1242/jeb.153379

sLEOD. Fig. 5 shows an example representative of nine units in which we had enough recordings to construct steady-state curves of spike latencies. In both extremes of the rms sLEOD range studied, resistive and capacitive effects on the waveform of the sLEOD converge to what we could call 'nearly open' and 'nearly short' circuits (Fig. 5A,B).

Accordingly, spike latencies in the burst elicited by resistive and capacitive loads resembling nearly open and nearly short circuits also converge. In the mid-range, there is a large difference in sLEOD waveform between those caused by resistive and capacitive loads. When the probe was loaded with resistors ranging from 2.5 MΩ to 1 kΩ, latencies and intervals were well fitted by linearly decreasing functions of the rms sLEOD. Consistently, the number of spikes increased with the rms sLEOD (Fig. 5C, red symbols and lines). When the probe was loaded by a capacitor, latencies and intervals did not follow the rms sLEOD in a linear way but were well fitted by a convex curve having a minimum value around the rms value corresponding to 10 nF load and the number of spikes per burst was greatest (5) at 10 nF (Fig. 5C, blue symbols and lines). Although the relationships observed for capacitance and resistance are qualitatively similar to those observed in the stimulus space depicted in Fig. 5A, the maximum difference in spike latency occurred at 10 nF instead of at 3.3 nF where the sLEOD showed the largest waveform distortion. As capacitive loads change both the rms sLEOD and the waveform of the signal, the shift in the maximum location suggests that sLEOD waveform distortion and rms sLEOD have synergistic effects on receptor responses.

To separate the effects of waveform and stimulus energy, capacitive and resistive loads were paired for energy content by adding the necessary resistance in series to the resistor arm at the control box in 16 units. In these units, the responses to the pair 10 nF–10 kΩ were studied in detail by step-switching between the resistive and the capacitive loads and vice versa every 15 s. The raster plots (Fig. 6A) and histograms (Fig. 6B,C) show that capacitive stimuli cause greater receptor responses than resistive stimuli. Sign-rank tests indicate statistically significant differences between the parameters of the trains at steady state (i.e. 100 EODs before the next step, $P<0.001$ and $N=16$, for the three comparisons; Fig. 6E).

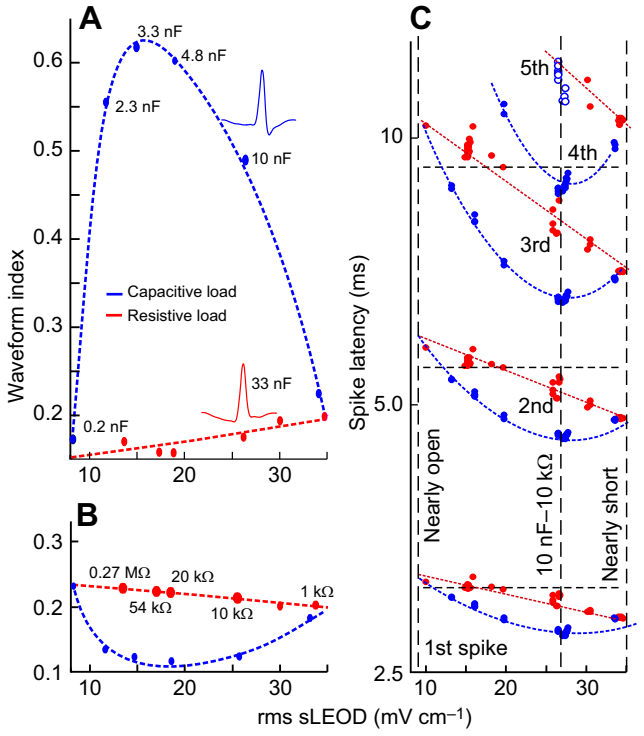

Fig. 5. Burst coder responses to different stimuli. (A,B) Plots of two waveform indices of stimuli plotted against their root mean square (rms) values (abscissa) when the probe object was loaded with capacitors (blue lines and symbols) or resistors (red lines and symbols) of different values. The two waveform indices were constructed from the early negative (sV1; B) and late negative (sV4; A) peaks measured as a fraction of the positive peak (sV3). (C) Spike latencies obtained from a receptor recorded in the same fish as the stimulus waveforms analyzed in A and B. Note that while the increase in stimulus energy caused by resistive loads determines a linear reduction in spike latency, the same increase in energy caused by a capacitive load determines more reduction in spike latency at intermediate values, with a maximum at stimulus amplitudes corresponding to 10 nF where only the capacitive load triggers a 5th spike (open symbols). For the sake of clarity, capacitance values are given in A and resistance values are given in B; the dashed lines in C are references for comparison with A and B.

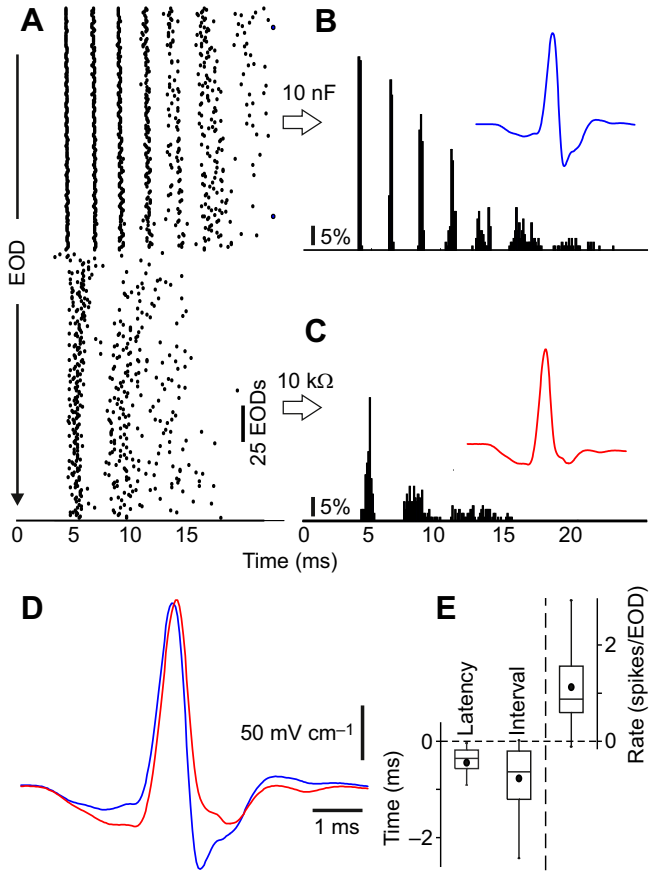

Fig. 6. Stepping between capacitive and resistive stimuli. (A–C) The raster plot (A) and corresponding post-EOD histograms taken after the burst parameters were stabilized (B,C) show a marked change after a step from a capacitive to a resistive object load when the loading resistance caused the same stimulus rms value as the capacitance. (D) Enlarged and superimposed version of the insets in A and B comparing the waveforms of the stimuli corresponding to resistive (red) and capacitive (blue) loads. (E) Box (25–75%) and whisker (5–95%) plots of the differences between (i) the latencies of the first spike, (ii) first interspike interval and (iii) the number of spikes per EOD obtained from 16 receptors in which this experiment was performed (first spike latencies: capacitive 3.2+0.78 ms versus resistive 3.64+0.97 ms, sign-rank test: $P=0.00043$, $N=16$; first interspike interval: capacitive 2.19+1.02 ms versus resistive 2.95+1.44 ms, sign-rank test: $P=0.00051$, $N=16$; and number of spikes per EOD: capacitive 3.64+1.12 versus resistive 2.51+0.81, sign-rank test: $P=0.0005$, $N=16$, Bonferroni correction).

Journal of Experimental Biology (2017) 220, 1663-1673 doi:10.1242/jeb.153379

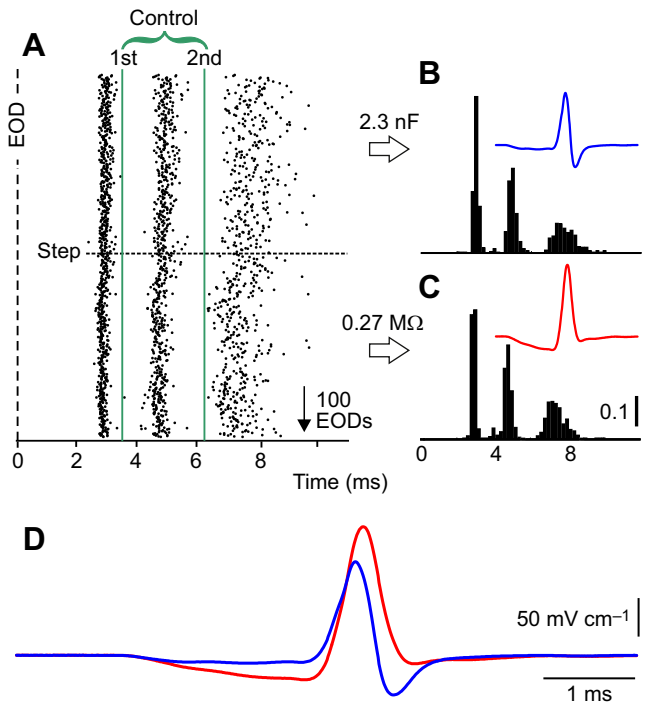

Fig. 7. Stepping between capacitive and resistive stimuli may cause little change in the response. (A–C) The raster (A) and the post-EOD histograms (B,C) of the unit essentially do not change after a step from a capacitive to a resistive object load when the resistance value has been adjusted to increase the amplitude of the sLEOD to compensate for the effect of waveform on the primary afferent responses. Green lines correspond to the mean response latencies of the same afferent in the absence of objects, showing that both stimuli are above threshold. (D) Superimposed stimuli caused by capacitive (blue) and resistive (red) loads showing the differences in waveform and amplitude of the signals.

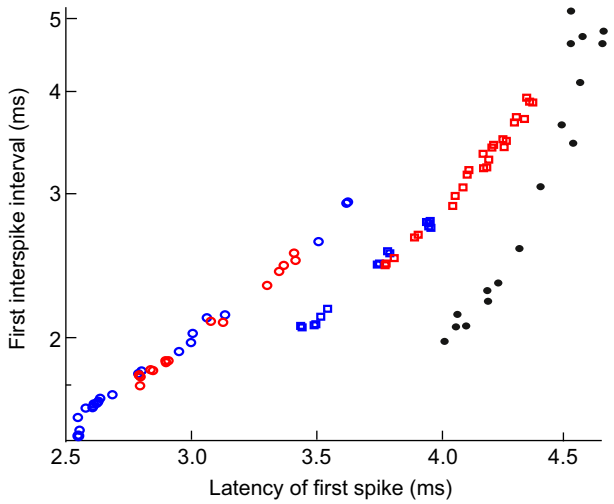

Fig. 8. Correlation between burst parameters. The plots of first interspike interval versus first spike latency obtained from two different receptors (squares and circles) stimulated with changes in probe impedance are compared with the data obtained in another experiment in which the object was moved. Statistical analysis for squares: capacitance (blue), r=0.99, r^2=0.98, slope=1.2, N=12; resistance (red), r=0.996, r^2=0.992, slope=0.94, N=27; circles: capacitance (blue), r=0.996, r^2=0.992, slope=0.8, N=20; resistance (red), r=0.995, r^2=0.99, slope=0.8, N=15; dots: r=0.95, r^2=0.90, N=20.

In three units, we were able to manipulate the resistor value using a potentiometer until the responses to resistive and capacitive loads were visually indistinguishable. The rms sLEOD required for matching the receptor responses was always larger for resistive loads (Fig. 7).

Finally, in six receptors, in which responses were recorded to more than six different capacitive and six different resistive stimuli, we studied the relationship between the parameters of the burst in order to determine whether the change in latency and interspike interval encode the same stimulus attribute. We found that the logarithm of the first interval was a linear function of the increment in latency of the first spike (coefficient of determination r^2>0.95 in all 12 cases; Fig. 8, red and blue dots). In addition, the linear relationship showed very similar slopes, with no significant differences between those corresponding to changes elicited by capacitive and resistive loads (sign-rank test, P=0.4, N=6). Data obtained with metal cylinders showed similar plots (r^2=0.90; Fig. 8, black dots).

DISCUSSION

The main finding of this work is that the subtype of primary afferent known as burst duration coders of *G. omarorum* is highly sensitive to EOD waveform distortion. The significance of our findings is discussed from three points of view: (1) the encoding properties of burst duration coders; (2) their ability to respond one-to-one to the EOD; and (3) the importance of waveform distortion sensitivity for electrosensory processing.

What are the encoding and encoded variables?

Changes in spike latency, interspike interval and spike number per EOD are well correlated. The coefficients of determination (r^2 values) indicate that more than 98% of the variance of the logarithm of the interval is explained by the variance of the latency. Also, the number of spikes increased stepwise with the decrease in latency and interval. Taking into account that the responses of the neurons of the electrosensory lobe are characterized by their post-EOD probability of firing (Pereira et al., 2014), one might postulate that all three parameters alone or combined (with different weight for different neurons) are important for synergistically driving the activity of downstream neurons in the ELL. However, the eponymous variable, duration, does not appear to be so important for image encoding.

Burst parameter correlations also indicate that they encode a single variable embedded in the sLEOD. This variable should express a combination of amplitude and phase of the different sLEOD frequency components. Heuristic modeling of receptor responsiveness (Cilleruelo and Caputi, 2012) accounts for previous data (Bastian, 1976, 1977; Bennett, 1971; McKibben et al., 1993; Yager and Hopkins, 1993; Watson and Bastian, 1979). Such a model, consisting of four stages (high-pass filtering, resonance, rectification and pulse encoding; Cilleruelo and Caputi, 2012) predicts the sensitivity of receptors to distortions in the amplitude and phase spectra of the natural stimulus waveform.

The large change in response observed in our study when provoking a distortion in the power spectra without changing the total energy of the sLEOD is in agreement with previous studies (Bastian, 1976, 1977; McKibben et al., 1993; Yager and Hopkins, 1993; Watson and Bastian, 1979) that showed that the threshold of burst duration coders is frequency dependent. Consistent with behavioral data (Aguilera and Caputi, 2003), we found that a specific range of capacitance (10–16 nF) causes the largest electroreceptor response. As this capacitive load evoked a large change in stimulus waveform and amplitude, this finding may correspond to the tuning curves that were used to distinguish

Journal of Experimental Biology

Journal of Experimental Biology (2017) 220, 1663-1673 doi:10.1242/jeb.153379

between electroreceptor subtypes (Bastian, 1976, 1977; McKibben et al., 1993; Watson and Bastian, 1979). However, in contrast to our study, which was done in self-discharging fish, these previous studies (McKibben et al., 1993; Watson and Bastian, 1979) were performed using harmonic analysis in curarized fish and the tuning curves were based on the threshold of the first spike. Therefore, our data evaluating how the burst parameters change with the presence of objects cannot be quantitatively compared with the findings of these previous studies. Moreover, a previous report in the same genus suggests that burst duration coder subtypes cannot be distinguished on the basis of best frequency or threshold at best frequency because these parameters are widely distributed in both classes (Watson and Bastian, 1979).

The additional role of the relative phases amongst the frequency components of the EOD waveform was also postulated theoretically (Cilleruelo and Caputi, 2012). However, in the case of our experiments, capacitance provokes a non-independent change of amplitude and phase of such components and, therefore, further reductionist studies independently altering phase and amplitude of the waveform frequency components would be required to pinpoint their relative roles in receptor responsiveness.

Finally, an important property found in our study is the adaptation of the response characterized by a fast initial stage followed by a long-lasting approach to a steady state. This adaptation time course clearly departs from an exponential function and resembles the power law adaptation observed in wave fish (Benda et al., 2005; Clarke et al., 2015). This property was not predicted by the heuristic model mentioned above (Cilleruelo and Caputi, 2012), although it can be compatible with a change in the synaptic properties between the receptor cells and the nerve terminals.

Electroreceptor responses indicate 'frame-to-frame' processing of electric images

Our results confirm previous findings (Bastian, 1976, 1977; Fessard and Szabo, 1961; Hagiwara and Morita, 1963; McKibben et al., 1993; Watson and Bastian, 1979; Yager and Hopkins, 1993) that both the pulse markers and burst duration coders encode every sLEOD either as single spike latency or as a burst of spikes. Although the number of spikes following each EOD may encode electric images in a relatively similar way to that in wave fish, the precise modulation of latency and interspike interval in the burst observed in our study may suggest that pulse fish more precisely encode the local signals. To maintain this resolution within behavioral requirements, these fish appear to have evolved precise control of EOD rate to adapt the inter-EOD interval (about 10 times longer in pulse than in wave fish) to changes in electric images with fish motor actions and environmental variations. The phasic–tonic response to changes in local stimulus observed in *G. omarorum* together with the 'frame-to-frame' signal evaluation may facilitate the detection of novel features in the electric images and contribute to the typical novelty responses elicited by changes in the electric image carried by a single EOD (Caputi et al., 2003).

Frame-to-frame evaluation of electrosensory images at the first processing stage concurs with electrophysiological data indicating that the electrosensory lobe neurons show characteristic post-EOD spike histograms (Pereira et al., 2014). This frame-to-frame image processing strategy is similar to what occurs in pulse fish of the evolutionarily distant mormyridae (Bell, 1990a,b; von der Emde and Bleckmann, 1992), but different from what is observed in the evolutionarily close wave gymnotiforms, which show an inter-EOD interval shorter than the time required for primary afferent spikes to reach the electrosensory lobe. This delay, together with the effects of adaptation, results in the well-known probability code of wave fish wherein increasing stimulus amplitude increases the spike probability of the primary afferents (Chacron et al., 2005; Krahe and Maler, 2014).

Sensory consequences of the sensitivity to stimulus waveform

Previous studies (Watson and Bastian, 1979) suggested that the waveform of the basal stimulus in the absence of objects is the optimal stimulus waveform. However, this does not appear to be the case as this stimulus is nearly at the mid-range of our experiments when the probe was loaded by a resistive stimulus. Moreover, waveform distortions elicited by capacitive loads cause a stronger response than the same changes in amplitude without a change in waveform elicited by resistive loads (Figs 5–7). This differential response to resistivity and capacitance may be behaviorally important for three reasons.

First, in pulse gymnotiforms, the self-generated electric field polarizing the nearby objects in the near environment has a different waveform depending upon object location relative to the body (Assad et al., 1999; Caputi et al., 1989, 1994, 1998a; Castelló et al., 2009; Rodríguez-Cattáneo et al., 2008, 2013; Stoddard et al., 1999; Waddell et al., 2016). The site-specific waveform is due to the different weight of the different waveforms emitted by the different regions of the electric organ (Caputi et al., 1989, 1994, 1998a; Rodríguez-Cattáneo et al., 2008, 2013; Castelló et al., 2009; Sanguinetti-Scheck et al., 2011; Pedraja et al., 2014; Waddell et al., 2016). Therefore, the presence of a large object on the side of the fish acts differently on the different EOD components generated by different regions of the fish's body. The waveform distortion sensitivity found here may serve to enhance the range of detection and spatial precision for localizing large objects in the peripheral electrosensory field (i.e. the body region of the electrosensory mosaic).

Second, because the waveform of the sLEOD of *G. omarorum* is relatively uniform throughout the foveal region at the anterior tip of the fish's body, local waveform distortions here may indicate the presence of a capacitive load and the changes in waveform may therefore be important for classifying objects (Aguilera and Caputi, 2003). While both resistive and capacitive load to an object probe change the amplitude of the local stimulus, only capacitive ones elicit large waveform phase and frequency distortions. Therefore, large changes in waveform of an object facing the fovea may be a clue for detecting a living prey, as living objects have more capacitance than non-living objects (von der Emde, 1990).

Finally, conspecific-generated LEODs (cLEODs) are characterized by a similar V4/V1 ratio to those changes caused by capacitance (Aguilera et al., 2001; Rodríguez-Cattáneo et al., 2008). In fact, sLEOD modulation by capacitive objects and cLEOD signals received by electroreceptors are characterized by an increase in the late negative wave (V4) and a reduction of the early smooth negative component (V1; Aguilera et al., 2001; Aguilera and Caputi, 2003). In addition, the waveform of the conspecific-generated signals changes with the relative position between fish (Aguilera et al., 2001). By analyzing the spatial profile of waveforms generated by a conspecific stimulating different receptors along the body, the fish may have clues for detecting conspecific position and relative orientation (Aguilera et al., 2001). Furthermore, in other pulse electric fish, such as some species of the genus *Brachyhypopomus*, there are transient, circadian and annual variations in far-field EOD waveform related to mating and dominance behaviors (Franchina and Stoddard, 1998; Franchina

et al., 2001; Perrone et al., 2009; Migliaro and Silva, 2016). The presence of phase-frequency distortion sensitivity of receptors and their hormonal modulation should be investigated to evaluate their potential role in such social behaviors.

In conclusion, the present study shows that the so-called burst duration coder electroreceptive afferents of pulse-type gymotiform electric fish are highly sensitive to phase-frequency distortion of the sLEOD waveform. Seminal work in gymnotiform electric fish with wave-type discharges (Bastian, 1981; Heiligenberg and Dye, 1982; Hopkins, 1976) showed how temporal and amplitude features of the self-generated signal waveform are encoded by different peripheral receptors. Further studies indicate that amplitude and time signals are separated into different paths at the periphery but re-integrated at higher brain levels to perform a quadrature analysis of phase and amplitude (reviewed in Carr and Maler, 1986; Heiligenberg, 1991; Kawasaki, 1997). The phase-frequency distortion sensitivity found here suggests that the fast and slow electrosensory paths of pulse fish may have differences from the homologous amplitude and time coding paths of wave fish. The burst parameters (latency of the first spike, first interspike interval and number of spikes) are well correlated between them, suggesting that they may contribute synergistically for driving downstream neurons and that they encode a single parameter which is modulated by both the amplitude and phase distortion of the stimulus. Waveform distortion sensitivity may contribute to enhance electroreceptive range in the peripheral 'electrosensory field' as well as to the better identification of the impedance of living prey and the presence and orientation of conspecifics.

Acknowledgements
The authors thank Dr Curtis Bell for critical comments and suggestions and English editing of the manuscript.

Competing interests
The authors declare no competing or financial interests.

Author contributions
Study Design: A.A.C.; Experiments: A.A.C., P.A.A., A.R.-C. Data Analysis: A.R.-C., P.A.A., A.A.C.; Manuscript writing: A.A.C., P.A.A., A.R.-C.

Funding
This research was partially funded by the National Agency for Research and Innovation (ANII: PhD fellowship to A.R.-C., SNI grants to P.A.A.); Universidad de la República del Uruguay (UDELAR: PhD fellowship complement to A.R.-C.); and Programa de Desarrollo de las Ciencias Básicas (PEDECIBA: research grants to A.A.C. and P.A.A.).

References
Aguilera, P. A. and Caputi, A. A. (2003). Electroreception in *G. carapo*: detection of changes in waveform of the electrosensory signals. *J. Exp. Biol.* **206**, 989-998.

Aguilera, P. A., Castelló, M. E. and Caputi, A. A. (2001). Electroreception in *Gymnotus carapo*: differences between self-generated and conspecific generated signal carriers. *J. Exp. Biol.* **204**, 185-198.

Assad, C., Rasnow, B. and Stoddard, P. K. (1999). Electric organ discharges and electric images during electrolocation. *J. Exp. Biol.* **202**, 1185-1193.

Aumentado-Armstrong, T., Metzen, M. G., Sproule, M. K. J. and Chacron, M. J. (2015). Electrosensory midbrain neurons display feature invariant responses to natural communication stimuli. *PLoS Comput. Biol.* **11**, e1004430.

Bastian, J. (1976). Frequency response characteristics of electroreceptors in weakly electric fish (gymnotoidei) with a pulse discharge. *J. Comp. Physiol. A* **112**, 165-180.

Bastian, J. (1977). Variations in the frequency response of electroreceptors dependent on receptor location in weakly electric fish (gymnotoidei) with a pulse discharge. *J. Comp. Physiol. A* **121**, 53-64.

Bastian, J. (1981). Electrolocation I. How the electroreceptors of *Apteronotus albifrons* code for moving objects and other electrical stimuli. *J. Comp. Physiol. A* **144**, 465-479.

Bell, C. C. (1990a). Mormyromast electroreceptor organs and their afferent fibers in mormyrid fish II. intra-axonal recordings show initial stages of central processing. *J. Neurophysiol.* **63**, 303-318.

Bell, C. (1990b). Mormyromast electroreceptor organs and their afferent fibers in mormyrid fish. III. Physiological differences between two morphological types of fibers. *J. Neurophysiol.* **63**, 319-332.

Bell, C. and Grant, K. (1989). Corollary discharge inhibition and preservation of temporal information in a sensory nucleus of mormyrid electric fish. *J. Neurosci.* **9**, 1029-1044.

Bell, C. C. and Maler, L. (2005). Central neuroanatomy of electrosensory systems in fish. In *Electroreception* (ed. T. Holmes Bullock, C. D. Hopkins and R. R. Fay), pp. 68-111. New York: Springer.

Bell, C. C., Zakon, H. and Finger, T. E. (1989). Mormyromast electroreceptor organs and their afferent fibers in mormyrid fish: I. Morphology. *J. Comp. Neurol.* **286**, 391-407.

Benda, J., Longtin, A. and Maler, L. (2005). Spike-frequency adaptation separates transient communication signals from background oscillations. *J. Neurosci.* **25**, 2312-2321.

Benda, J., Longtin, A. and Maler, L. (2006). A synchronization-desynchronization code for natural communication signals. *Neuron* **52**, 347-358.

Bennett, M. V. L. (1971). Electroreception. *Fish Physiol.* **5**, 493-574.

Budelli, R. and Caputi, A. A. (2000). The electric image in weakly electric fish: perception of objects of complex impedance. *J. Exp. Biol.* **203**, 481-492.

Bullock, T. H., Hagiwara, S., Kusano, K. and Negishi, K. (1961). Evidence of a category of electroreceptors in the lateral line of gymnotid fishes. *Science* **134**, 1426-1427.

Caputi, A. and Budelli, R. (1995). The electric image in weakly electric fish: I. A data-based model of waveform generation in *Gymnotus carapo*. *J. Comput. Neurosci.* **2.2**, 131-147.

Caputi, A., Macadar, O. and Trujillo-Cenóz, O. (1989). Waveform generation of the electric organ discharge in *Gymnotus carapo*. *J. Comp. Physiol. A* **165**, 361-370.

Caputi, A., Macadar, O. and Trujillo-Cenóz, O. (1994). Waveform generation in *Rhamphichthys rostratus* (L.) (Teleostei, Gymnotiformes). *J. Comp. Physiol. A* **174**, 633-642.

Caputi, A. A., Silva, A. C. and Macadar, O. (1998a). The electric organ discharge of *Brachyhypopomus pinnicaudatus*. *Brain Behav. Evol.* **52**, 148-158.

Caputi, A., Budelli, R., Grant, K. and Bell, C. (1998b). The electric image in weakly electric fish: physical images of resistive objects in *Gnathonemus petersii*. *J. Exp. Biol.* **201**, 2115-2128.

Caputi, A. A., Castelló, M. E., Aguilera, P. and Trujillo-Cenóz, O. (2002). Electrolocation and electrocommunication in pulse gymnotids: signal carriers, pre-receptor mechanisms and the electrosensory mosaic. *J. Physiol. Paris* **96**, 493-505.

Caputi, A. A., Aguilera, P. and Castelló, M. E. (2003). Probability and amplitude of novelty responses as a function of the change in contrast of the reafferent image in *G.* carapo. *J. Exp. Biol.* **206**, 989-998.

Caputi, A. A., Aguilera, P. A. and Pereira, A. C. (2011). Active electric imaging: body-object interplay and object's "electric texture". *PLoS ONE* **6**, e22793.

Carr, C. E. and Maler, L. (1986). Electroreception in gumnotiform fish. Central anatomy and physiology. In *Electroreption* (ed. T. H. Bullock and W. Heiligenberg), pp. 319-373. New York: Wiley.

Castello, M. E., Caputi, A. and Trujillo-Cenòz, O. (1998). Structural and functional aspects of the fast electrosensory pathway in the electrosensory lateral line lobe of the pulse fish *Gymnotus carapo*. *J. Comp. Neurol.* **401**, 549-563.

Castello, M. E., Aguilera, P. A., Trujillo-Cenòz, O. and Caputi, A. A. (2000). Electroreception in *Gymnotus carapo*: pre-receptor processing and the distribution of electroreceptor types. *J. Exp. Biol.* **203**, 3279-3287.

Castelló, M. E., Rodríguez-Cattáneo, A., Aguilera, P. A., Iribarne, L., Pereira, A. C. and Caputi, A. A. (2009). Waveform generation in the weakly electric fish *Gymnotus coropinae* (Hoedeman): the electric organ and the electric organ discharge. *J. Exp. Biol.* **212**, 1351-1364.

Chacron, M. J., Longtin, A., St-Hilaire, M. and Maler, L. (2000). Suprathreshold stochastic firing dynamics with memory in p-type electroreceptors. *Phys. Rev. Lett.* **85**, 1576.

Chacron, M. J., Maler, L. and Bastian, J. (2005). Electroreceptor neuron dynamics shape information transmission. *Nat. Neurosci.* **8**, 673-678.

Cilleruelo, E. R. and Caputi, A. (2012). Encoding electric signals by gymnotus omarorum: heuristic modeling of tuberous electroreceptor organs. *Brain Res.* **1434**, 102-114.

Clarke, S. E., Longtin, A. and Maler, L. (2015). Contrast coding in the electrosensory system: parallels with visual computation. *Nat. Rev. Neurosci.* **16**, 733-744.

Clarke, S. E., Longtin, A. and Maler, L. (2015). The neural dynamics of sensory focus. *Nat. Commun.* **6**, 8764.

Coates, C. W., Altamirano, M. and Grundfest, H. (1954). Activity in electrogenic organs of knifefishes. *Science* **120**, 845-846.

Dye, J. and Meyer, J. (1986). Central control of the electric organ discharge in weakly electric fish. In *Electroreception* (ed. T. Holmes Bullock and W. Heiligenberg), pp. 71-102. New York: Wiley.

Echagüe, A. and Trujillo-Cenóz, O. (1980). Innervation patterns in the tuberous organs of *Gymnotus carapo*. Sensory Physiology of Aquatic Lower Vertebrates: Satellite Symposium of the 28th International Congress of Physiological Sciences, Keszthely, Hungary, 1980, Vol. 31, p. 29. Elsevier.

Fessard, A. and Szabo, T. (1961). Mise en évidence d'un récepteur sensible à l'électricité dans la peau des mormyres. *C. R. Acad. Sci.* **253**, 1859.
Franchina, C. R. and Stoddard, P. K. (1998). Plasticity of the electric organ discharge waveform of male *Brachyhypopomus pinnicaudatus*. I. Quantification of day-night changes. *J. Comp. Physiol. A* **183**, 759-768.
Franchina, C. R., Salazar, V. L., Volmar, C.-H. and Stoddard, P. K. (2001). Plasticity of the electric organ discharge waveform of male *Brachyhypopomus pinnicaudatus*. II. Social effects. *J. Comp. Physiol. A Sens. Neural Behav. Physiol.* **187**, 45-52.
Gómez, L., Budelli, R., Grant, K. and Caputi, A. A. (2004). Pre-receptor profile of sensory images and primary afferent neuronal representation in the mormyrid electrosensory system. *J. Exp. Biol.* **207**, 2443-2453.
Hagiwara, S. and Morita, H. (1963). Coding mechanisms of electroreceptor fibers in some electric fish. *J. Neurophysiol.* **26**, 551-567.
Harvey Girard, E., Tweedle, J., Ironstone, J., Cuddy, M., Ellis, W. and Maler, L. (2010). Long-term recognition memory of individual conspecifics is associated with telencephalic expression of Egr-1 in the electric fish *Apteronotus leptorhynchus*. *J. Comp. Neurol.* **518**, 2666-2692.
Heiligenberg, W. (1991). *Neural Nets in Electric Fish*, p. 179. Cambridge, MA: MIT press.
Heiligenberg, W. and Dye, J. (1982). Labelling of electroreceptive afferents in a gymnotoid fish by intracellular injection of HRP: the mystery of multiple maps. *J. Comp. Physiol. A* **148**, 287-296.
Heiligenberg, W. and Rose, G. (1985). Phase and amplitude computations in the midbrain of an electric fish: intracellular studies of neurons participating in the jamming avoidance response of Eigenmannia. *J. Neurosci.* **5**, 515-531.
Hopkins, C. D. (1976). Stimulus filtering and electroreception: tuberous electroreceptors in three species of Gymnotoid fish. *J. Comp. Physiol. A* **111**, 171-207.
Jun, J. J., Longtin, A. and Maler, L. (2014). Enhanced sensory sampling precedes self-initiated locomotion in an electric fish. *J. Exp. Biol.* **217**, 3615-3628.
Kawasaki, M. (1997). Sensory hyperacuity in the jamming avoidance response of weakly electric fish. *Curr. Opin. Neurobiol.* **7**, 473-479.
Kawasaki, M. (2005). Physiology of tuberous electrosensory systems. In *Electroreception* (ed. T. Holmes Bullock, C. D. Hopkins and R. R. Fay), pp. 154-194. New York: Springer.
Krahe, R. and Maler, L. (2014). Neural maps in the electrosensory system of weakly electric fish. *Curr. Opin. Neurobiol.* **24**, 13-21.
Lissmann, H. (1958). On the function and evolution of electric organs in fish. *J. Exp. Biol.* **35**, 156-191.
McKibben, J. R., Hopkins, C. D. and Yager, D. D. (1993). Directional sensitivity of tuberous electroreceptors: polarity preferences and frequency tuning. *J. Comp. Physiol. A* **173**, 415-424.
Meyer, J. H. (1982). Behavioral responses of weakly electric fish to complex impedances. *J. Comp. Physiol. A* **145**, 459-470.
Migliaro, A. and Silva, A. (2016). Melatonin regulates daily variations in electric behavior arousal in two species of weakly electric fish with different social structures. *Brain Behav. Evol.* **87**, 232-241.
Moller, P. (1995). *Electric Fishes: History and Behavior*, Vol. 17. London: Chapman & Hall.
Neiffer, D. L. and Stamper, M. A. (2009). Fish sedation, anesthesia, analgesia, and euthanasia: considerations, methods, and types of drugs. *ILAR J.* **50**, 343-360.
Pedraja, F., Aguilera, P., Caputi, A. A. and Budelli, R. (2014). Electric imaging through evolution, a modeling study of commonalities and differences. *PLOS Comput. Biol.* **10**, e1003722.
Pereira, A. C., Rodríguez-Cattáneo, A. and Caputi, A. A. (2014). The slow pathway in the electrosensory lobe of gymnotus omarorum: field potentials and unitary activity. *J. Physiol.-Paris* **108**, 71-83.
Perrone, R., Macadar, O. and Silva, A. (2009). Social electric signals in freely moving dyads of *Brachyhypopomus pinnicaudatus*. *J. Comp. Physiol. A* **195**, 501-514.
Post, N. and von der Emde, G. (1999). The "novelty response" in an electric fish: response properties and habituation. *Physiol. Behav.* **68**, 115-128.
Rodríguez-Cattáneo, A., Pereira, A. C., Aguilera, P. A., Crampton, W. G. R. and Caputi, A. A. (2008). Species-specific diversity of a fixed motor pattern: the electric organ discharge of Gymnotus. *PLoS ONE* **3**, e2038.
Rodríguez-Cattáneo, A., Aguilera, P., Cilleruelo, E., Crampton, W. G. R. and Caputi, A. A. (2013). Electric organ discharge diversity in the genus Gymnotus: anatomo-functional groups and electrogenic mechanisms. *J. Exp. Biol.* **216**, 1501-1515.
Sanguinetti-Scheck, J. I., Pedraja, E. F., Cilleruelo, E., Migliaro, A., Aguilera, P., Caputi, A. A. and Budelli, R. (2011). Fish geometry and electric organ discharge determine functional organization of the electrosensory epithelium. *PLoS ONE* **6**, e27470.
Sawtell, N. B., Williams, A., Roberts, P. D., von der Emde, G. and Bell, C. C. (2006). Effects of sensing behavior on a latency code. *J. Neurosci.* **26**, 8221-8234.
Scheich, H. and Bullock, T. H. (1974). The detection of electric fields from electric organs. In *Electroreceptors and Other Specialized Receptors in Lower Vertrebrates* (ed. A. Fessard), pp. 201-256. Heidelberg: Springer.
Schumacher, S., de Perera, T. B., Thenert, J. and von der Emde, G. (2016). Cross-modal object recognition and dynamic weighting of sensory inputs in a fish. *Proc. Natl. Acad. Sci. USA* **113**, 7638-7643.
Stoddard, P. K., Rasnow, B. and Assad, C. (1999). Electric organ discharges of the gymnotiform fishes: III. Brachyhypopomus. *J. Comp. Physiol. A* **184**, 609-630.
Szabo, T. (1974). Anatomy of the specialized lateral line organs of electroreception. In *Electroreceptors and Other Specialized Receptors in Lower Vertrebrates* (ed. A. Fessard), pp. 13-58. Heidelberg: Springer.
Szabo, T. and Fessard, A. (1974). Physiology of electroreceptors. In *Electroreceptors and Other Specialized Receptors in Lower Vertrebrates* (ed. A. Fessard), pp. 59-124. Heidelberg: Springer.
Szabo, T., Sakata, H. and Ravaille, M. (1975). An electrotonically coupled pathway in the central nervous system of some teleost fish, Gymnotidae and Mormyridae. *Brain Res.* **95**, 459-474.
Trinh, A.-T., Harvey-Girard, E., Teixeira, F. and Maler, L. (2016). Cryptic laminar and columnar organization in the dorsolateral pallium of a weakly electric fish. *J. Comp. Neurol.* **524**, 408-428.
Trujillo-Cenóz, O., Echagüe, J. A. and Macadar, . O. (1984). Innervation pattern and electric organ discharge waveform in *Gymnotus carapo* (Teleostei; Gymnotiformes). *J. Neurobiol.* **15**, 273-281.
von der Emde, G. (1990). Discrimination of objects through electrolocation in the weakly electric fish, gnathonemus petersii. *J. Comp. Physiol. A* **167**, 413-421.
von der Emde, G. and Bell, C. C. (1994). Responses of cells in the mormyrid electrosensory lobe to EODs with distorted waveforms: implications for capacitance detection. *J. Comp. Physiol. A* **175**, 83-93.
von der Emde, G. and Bleckmann, H. (1992). Differential responses of two types of electroreceptive afferents to signal distortions may permit capacitance measurement in a weakly electric fish, Gnathonemus petersii. *J. Comp. Physiol. A* **171**, 683-694.
von der Emde, G. and Ronacher, B. (1994). Perception of electric properties of objects in electrolocating weakly electric fish: two-dimensional similarity scaling reveals a city-block metric. *J. Comp. Physiol. A* **175**, 801-812.
Waddell, J. C., Rodríguez-Cattáneo, A., Caputi, A. A. and Crampton, W. G. R. (2016). Electric organ discharges and near-field spatiotemporal patterns of the electromotive force in a sympatric assemblage of Neotropical electric knifefish. *J. Physiol.-Paris*.
Walton, A. G. and Moller, P. (2010). Maze learning and recall in a weakly electric fish, Mormyrus rume proboscirostris Boulenger (Mormyridae, Teleostei) 1. *Ethology* **116**, 904-919.
Watson, D. and Bastian, J. (1979). Frequency response characteristics of electroreceptors in the weakly electric fish, gymnotus carapo. *J. Comp. Physiol. A* **134**, 191-202.
Wright, P. G. (1958). An electrical receptor in fishes. *Nature* **181**, 64-65.
Yager, D. D. and Hopkins, C. D. (1993). Directional characteristics of tuberous electroreceptors in the weakly electric fish, hypopomus (gymnotiformes). *J. Comp. Physiol. A* **173**, 401-414.
Zakon, H. H. (1986). The electroreceptive periphery. In *Electroreception* (ed. T. Holmes Bullock and W. Heiligenberg), pp. 103-156. New York: Wiley.